


## Molecularly imprinted nanoparticles with recognition properties towards diphtheria toxin for ELISA applications

Süleyman Serdar Alkanlı, Fulya Dal Yöntem, Merve Yaşar, Celal Güven, M. Vezir Kahraman, Nilhan Kayaman Apohan, Zerrin Aktaş, Mustafa Oral Öncül, Ayhan Ünlü & Handan Akçakaya


To cite this article: Süleyman Serdar Alkanlı, Fulya Dal Yöntem, Merve Yaşar, Celal Güven, M. Vezir Kahraman, Nilhan Kayaman Apohan, Zerrin Aktaş, Mustafa Oral Öncül, Ayhan Ünlü & Handan Akçakaya (2022): Molecularly imprinted nanoparticles with recognition properties towards diphtheria toxin for ELISA applications, Journal of Biomaterials Science, Polymer Edition, DOI: [10.1080/09205063.2022.2145866](https://doi.org/10.1080/09205063.2022.2145866)

To link to this article: <https://doi.org/10.1080/09205063.2022.2145866>

 View supplementary material [↗](#)

 Published online: 17 Nov 2022.

 Submit your article to this journal [↗](#)










 Article views: 44

 View related articles [↗](#)

 View Crossmark data [↗](#)



## Molecularly imprinted nanoparticles with recognition properties towards diphtheria toxin for ELISA applications

Süleyman Serdar Alkanlı<sup>a,b</sup> , Fulya Dal Yöntem<sup>c,d</sup> , Merve Yaşar<sup>e</sup> ,  
Celal Güven<sup>f</sup> , M. Vezir Kahraman<sup>e</sup> , Nilhan Kayaman Apohan<sup>e</sup> ,  
Zerrin Aktaş<sup>g</sup> , Mustafa Oral Öncül<sup>h</sup> , Ayhan Ünlü<sup>i</sup>  and  
Handan Akçakaya<sup>a</sup> 

<sup>a</sup>Department of Biophysics, Istanbul Faculty of Medicine, Istanbul University, Istanbul, Turkey; <sup>b</sup>Department of Biophysics, Institute of Health Sciences, Istanbul Faculty of Medicine, Istanbul University, Istanbul, Turkey; <sup>c</sup>Department of Biophysics, Koç University School of Medicine, Koç University, Istanbul, Turkey; <sup>d</sup>Koç University Research Center for Translational Medicine (KUTTAM), Istanbul, Turkey; <sup>e</sup>Department of Chemistry, Faculty of Art and Science, Marmara University, Göztepe, Istanbul, Turkey; <sup>f</sup>Department of Biophysics, Faculty of Medicine, Adiyaman University, Adiyaman, Turkey; <sup>g</sup>Department of Microbiology & Clinical Microbiology, Istanbul Faculty of Medicine, Istanbul University, Istanbul, Turkey; <sup>h</sup>Department of Infectious Diseases & Clinical Microbiology, Istanbul Faculty of Medicine, Istanbul University, Istanbul, Turkey; <sup>i</sup>Department of Biophysics, Faculty of Medicine, Trakya University, Edirne, Turkey

### ABSTRACT

Plastic antibodies can be used for *in vitro* neutralization of biomacromolecules with different fragments due to their potential in separation, purification, chemical sensor, catalysis and drug production studies. These polymer nanoparticles with binding affinity and selectivity comparable to natural antibodies were prepared using functional monomer synthesis and copolymerization of acrylic monomers *via* miniemulsion polymerization. As a result, the *in vitro* cytotoxic effect from diphtheria toxin was reduced by MIPs. *In vitro* imaging experiments of polymer nanoparticles (plastic antibodies) were performed to examine the interaction of diphtheria toxin with actin filaments, and MIPs inhibited diphtheria toxin damage on actin filaments. The enzyme-linked immunosorbent assay (ELISA) was performed with plastic antibodies labeled with biotin, and it was determined that plastic antibodies could also be used for diagnostic purposes. We report that molecularly imprinted polymers (MIPs), which are biocompatible polymer nanoparticles, can capture and reduce the effect of diphtheria toxin and its fragment A.

### HIGHLIGHTS

- Macromolecules can be imprinted by using their fragments as template molecules.
- MIPs gain an affinity for the template molecule by covalent binding, non-covalent interactions or ligand interactions, as well as the ability to bind, release and recognize the template molecule.

### ARTICLE HISTORY

Received 30 July 2022  
Accepted 7 November 2022

### KEYWORDS

Molecularly imprinted polymer; plastic antibody; diphtheria toxin; ELISA

- The viability of cells treated with DT, NIPs and MIPs was determined by MTT assay.
- Immunofluorescence staining studies examined structural changes in actin filaments in HUVEC treated with DT, NIPs and MIPs.
- FA imprinted polymer has the ability to bind whole diphtheria toxin.
- FA-MIP gave significant results in terms of specificity in ELISA using diphtheria toxin.

## 1. Introduction

MIPs are synthetic receptors [1] that can be used in the recognition and binding of a large number of molecules. MIPs have the potential to replace natural antibodies in terms of their binding affinity and specificity to the template molecule. For this reason, they are also called plastic antibodies [2]. In addition to the difficulties of natural antibodies such as complex production processes and long production times, different types of animals (rats, mice, rabbits, goats, etc.) are also needed for their production. Therefore, new approaches have emerged, and it has become attractive to develop MIPs that are easy to produce, low in cost and reusable [1–3]. MIPs gain an affinity for the template molecule by covalent binding, non-covalent interactions or ligand interactions, as well as the ability to bind, release and recognize the template molecule. Because of these properties, they can be used in separation, purification, chemical sensor, catalysis, and drug production studies [4].

Although small template molecules can be imprinted, there are some technical difficulties in the imprinting of macromolecules. Macromolecules are incompatible with organic solvents therefore the polymerization process must be carried out in an aqueous solution [5–8]. Epitope imprinting approach, which is a molecular imprinting method, can produce MIPs with high affinity for the target macromolecule by using fragments of macromolecules [9–12]. Diphtheria toxin (DT), a macromolecule with A-B fragments, is secreted by *Corynebacterium diphtheria* bacterium and enters the cell by endocytosis and then causes diphtheria, a respiratory tract and skin disease. DT consists of receptor-binding (R-), transmembrane (T-), and catalytic (C-) domains. The C-domain, which is an independent folding domain, forms fragment A (FA), and the T- and R-domains form fragment B (FB) [13,14]. The R-domain binds to the cell surface receptors such as epidermal growth factor receptor (EGFR), allowing DT to enter the cell by endocytosis. T-domain inserts into the membrane after decrease of pH in the endosome interior. T-domain has a monomeric globular form comprised of ten  $\alpha$ -helices at neutral pH (pH: 7.0). In the presence of anionic bilayers and acidity, the protein undergoes conformational changes. T-domain assists membrane insertion and translocation of C-domain across the endosome membrane into the cytosol [15]. The C-domain is then proteolyzed from the R- and T-domains. The C-domain reaching the cytosol inhibits the eukaryotic elongation factor 2 (eEF2) translation factor, ending protein synthesis and causing cell death [13–16]. FA inhibits globular G-actin polymerization and initiates depolymerization of filamentous F-actin [17–19].

In our study, we aimed to bind the entire DT macromolecule by using the FA template molecule imprinted plastic antibody. Since aqueous media are preferred for imprinting, MIPs were prepared by miniemulsion polymerization technique. Allyl N,N-diallyl phenylalaninate (TAPA), N-[3-(N,N-dimethylamino)propyl] methacrylamide and N-hydroxyethyl acrylamide were preferred as functional monomers. Ethylene glycol dimethacrylate (EGDMA) was used as the crosslinker. Polymerization was carried out in water-in-oil-in-water W/O/W emulsions. The emulsion was stabilized using sodium dodecyl sulfate (SDS), poly (vinyl alcohol) (PVA) and hexadecane. In addition, non-imprinted polymer (NIP) without template molecule was prepared to determine the toxic effect of the polymer [20].

The cytotoxic effects of MIP, NIP and DT on human umbilical vein endothelial cells (HUVEC) were determined by cell viability assay. Changes in the actin filaments and cell nuclei of the cells were visualized by immunofluorescence staining [21–23].

In this study, we show that macromolecules can be imprinted by using their fragments as template molecules. This approach is applicable for many toxins with fragments and will provide a better understanding of molecular imprinting studies. It will also contribute to the literature by revealing the therapeutic use potential of MIPs.

## 2. Materials and methods

### 2.1. Reagents

DT was purchased from Sigma-Aldrich Co. (St. Louis, MO, USA). 2-hydroxyethyl methacrylate (HEMA), N-hydroxyethyl acrylamide, N-[3-(N,N-dimethylamino)propyl] methacrylamide, L-Phenylalanine, Allyl bromide, hexadecane, EGDMA, pentaerythritol tetrakis (3-mercaptopropionate), SDS and PVA (Mw: 31,000 and 88% hydrolyzed) were obtained from Sigma-Aldrich Co. (St. Louis, MO, USA). Camforquinone and 1-hydroxycyclohexyl phenyl ketone were used as photoinitiators and were purchased from Sigma-Aldrich Co. (St. Louis, MO, USA). 3-[4,5-dimethylthiazol-2-yl]-2,5-diphenyltetrazolium bromide; thiazolyl blue (MTT) solution was purchased from Alfa Aesar. 3,3',5,5'-Tetramethylbenzidine (TMB) and Sulfo-NHS-LC-Biotin were obtained from Thermo Fisher. HRP-streptavidin was purchased from Sigma-Aldrich Co. (St. Louis, MO, USA). Bovine Serum Albumin (BSA) was obtained from Capricorn.

### 2.2. Purification of fragment A

Commercially purchased DT was separated into A and B fragments using trypsin and dithiothreitol (DTT) to obtain the template molecule FA for molecular imprinting [24]. Four mg ml<sup>-1</sup> of trypsin was added to the solution with 50 mM Tris-HCl pH: 8.0 and 1 mM EDTA was used to obtain FA. The solution was diluted 1:1000 (4 mg ml<sup>-1</sup> trypsin). 5 μl of the solution was taken and 2 mg ml<sup>-1</sup> of DT solution was added. After incubation for 30 min at 25 °C, 0.1 M DTT was added to the mixture and then incubated at 37 °C for 90 min. To dissociate the FA and FB fragments of DT, the solution was treated with 0.6 μg ml<sup>-1</sup> trypsin inhibitor at 25 °C [25,26].

AKTA Prime Plus liquid chromatography device was used to obtain the FA after digestion. The device was calibrated with BSA [27]. A Hiprep 16/60 Sephacryl S-100

column with a total volume of 120 ml was used for purification. Then, digested DT was added into the liquid chromatography device, and FA was collected in fractions of 1 ml at a pressure of 0.37 mPa, at a rate of  $1 \text{ ml min}^{-1}$ . The peak values of FA and DT on the graph were checked by comparing them with the values on the chromatogram image.

### **2.3. SDS-PAGE and Western blot analysis**

Sodium dodecyl sulfate-polyacrylamide gel electrophoresis (SDS-PAGE) (4%–12%) and western blot were used to ensure digestion of DT. SDS-PAGE was performed according to the Laemmli method [28] and the gel was stained with Coomassie Brilliant Blue. In western blotting, the protein bands were transferred to a polyvinylidene difluoride (PVDF) membrane (Invitrogen) using iBlot® Gel Transfer Device (Invitrogen). Anti-diphtheria toxin FA specific mouse monoclonal antibody (Abcam) and an IgG conjugated secondary antibody (diluted 1:3000) were used to identify the protein bands. Bands were visualized in TMB solution. Protein concentration was determined using the buffer in the Qubit<sup>TM</sup> Protein Assay Kit (Invitrogen), which can calculate the sample range from 12.5 to  $5 \mu\text{g ml}^{-1}$  (According to the manufacturer's instructions).

### **2.4. Preparation of fragment A imprinted polymer nanoparticles**

FA imprinted MIPs (FA-MIP) were prepared by miniemulsion polymerization [29]. HEMA (0.4 g), N-hydroxyethyl acrylamide (0.45 g), N-[3-(N,N-dimethylamino)propyl] methacrylamide (0.1 g), TAPA (0.03 g) and hexadecane (0.03 g) were mixed and EGDMA (0.02 g) and pentaerythritol tetrakis (3-mercaptopropionate) (0.03 g) were added into this mixture. TAPA was synthesized similar to our previous publication [20]. To form an oil-in-water (O/W) emulsion into the resulting mixture; 0.6% (wt/vol) SDS, 0.3% (wt/vol)  $\text{NaHCO}_3$  and 2% (wt/vol) 0.1 g PVA were added and homogenized using an ultrasonic homogenizer (UP200Ht Hielscher) for 30 s at 25,000 rpm. The template molecule (FA,  $30 \mu\text{g ml}^{-1}$ ) was added to the O/W emulsion and mixed for 30 min to obtain a pre-polymerization complex. Then, 0.015 g of 1-hydroxycyclohexyl phenyl ketone and 0.015 g of camphorquinone were added as photoinitiators. To obtain W/O/W miniemulsion; The W/O emulsion was poured into 100 ml of a mixture of 0.05% (wt/vol) PVA and 0.1% (wt/vol) SDS. The mixture was stirred at 700 rpm using a magnetic stirrer and homogenized by an ultrasonic homogenizer for 30 s at 25,000 rpm.

The miniemulsion was placed in the photo-reactor (Luzchem's LZC-ICH2 photo-reactor) in a quartz reaction flask and the reaction mixture was stirred for 10 min to obtain FA-MIP. The imprinted nanoparticles were washed with 10% acetic acid solution and ethanol to remove unreacted monomers, initiator, and unbound FAs. The polymerized nanoparticle solution was purified by dialysis against distilled water (at least 3 times a day for 4 days) to remove FA from the nanoparticles. Non-imprinted nanoparticles (NIPs) were prepared using the same protocol without the template molecule.

## 2.5. Characterization studies

TAPA was characterized with Fourier Transform Infrared Spectroscopy (FTIR, Perkin Elmer ATR-FTIR spectrophotometer and Proton Nuclear Magnetic Resonance Spectroscopy ( $^1\text{H}$  NMR, Varian Gemini 400 MHz) for structural confirmations. The details were given in our previous paper [20].

Nanoparticle morphology was examined by using scanning transmission electron microscopy (STEM-Philips XL30 ESEM-FEG/EDAX North Billerica, MA). Nanoparticles were dissolved in water and a sample is placed on a grid. The sample was lyophilized and the nanoparticles were dried. The morphology of the dried nanoparticles was examined by Scanning electron microscopy (SEM). Approximately 300 Å gold plating was applied to the samples prepared by freeze fracturing in liquid nitrogen.

## 2.6. Cytotoxicity and neutralization studies

HUVEC purchased from the American Type Culture Collection (ATCC) were cultured in Dulbecco's Modified Eagle Medium (DMEM) (Gibco) containing 10% fetal bovine serum and 100 IU penicillin/streptomycin at 37 °C and 5% CO<sub>2</sub> incubator. For the cytotoxicity experiments,  $5 \times 10^4$  cells ml<sup>-1</sup> per well were seeded into 96-well culture plates and then treated with 5, 10, 50, 100, 500, 1000, 5000, 10000 ng ml<sup>-1</sup> DT for 24, 48 and 72 h at 37 °C and 5% CO<sub>2</sub>. After the indicated treatments 0.5 mg ml<sup>-1</sup> of MTT was added into each well and the plates were incubated at 37 °C and 5% CO<sub>2</sub>. The solution in each well was removed and 100 µl of dimethyl sulfoxide (DMSO) was added to the wells. Then, the plates were incubated for 30 min in the dark at room temperature. The cell viability was calculated by determining the absorbance values of the cells in the plate wells by UV/Visible microplate reader (Epoch, Biotek) at 570 nm wavelength. Experiments were performed in duplicate wells and were repeated at least three times. The same procedures were performed for NIP at 1, 2, 5, 10, 25, 50, and 100 µg ml<sup>-1</sup> concentrations.

In neutralization experiments, the DT neutralization efficiency of FA-MIP was investigated in HUVEC was seeded into each well of 96-well plates and cells were treated with 100 µg ml<sup>-1</sup> DT and 1, 2, 5, 10, 25, 50, 100 µg ml<sup>-1</sup> FA-MIP for 24, 48 and 72 h at 37 °C and 5% CO<sub>2</sub>. Cell viability was then determined by MTT. Experiments were performed in duplicate wells and were repeated at least three times.

## 2.7. Immunofluorescence staining

Bacterial toxins have ADP-ribosylation effects on the filamentous actin (F-actin) structure. Therefore, the morphological structures of F-actin in HUVEC were investigated. To examine the morphological effects of DT on F-actin of HUVEC 115,000 cells ml<sup>-1</sup> were seeded onto coverslip in each well of 6-well plates and cells were treated with 5, 500, 5000 ng ml<sup>-1</sup> DT for 24, 48 and 72 h at 37 °C and 5% CO<sub>2</sub>. After incubation, cells were washed with PBS and fixed with 2% paraformaldehyde for 1 h at room temperature. Then, the permeability of the cells was increased with 0.1% (v/v) Triton X-100 in PBS for 15 min. Afterward, cells were blocked with 5% BSA in

PBS for 60 min at room temperature. Next cells were washed 3 times with PBS and labeled with Alexa Flour 594 phalloidin for F-actin and 4',6-diamidino-2-phenylindole dichloride (DAPI) for nuclei. F-actin was visualized in Olympus DP2-TWAIN software using the DP72 camera in an Olympus BX51 microscope.

### **2.8. Biotin-FA-MIP/NIP conjugate and ELISA**

Sulfo-NHS-LC-Biotin (long chain biotin NHS ester, Thermo Fisher) was dissolved in ultrapure water to a final concentration of 10 mM according to the manufacturer. Biotin labeling process depends on the distribution of protein concentration, amount of reagent used distribution of amino groups on the protein [30]. Therefore, as the manufacturer suggests the equation below was used to determine the amount of biotin to be added onto MIP and NIP's:

$$\text{ml protein} \times \frac{\text{mg protein}}{\text{ml protein}} \times \frac{\text{mmol protein}}{\text{mg protein}} \times \frac{20 \text{ mmol Biotin}}{\text{mmol protein}} = \text{mmol Biotin}$$

After 1 h of incubation in dark at room temperature, biotin-labeled samples (FA-MIP or NIP) were dialyzed against PBS overnight at room temperature on a magnetic stirrer to remove unbound biotin.

Microplates were coated with FA or DT (100  $\mu\text{l}$ , 0.0021  $\text{mg ml}^{-1}$ ) into each well followed by overnight incubation at +4 °C. Each well was then conditioned by washing with PBS containing 0.05% Tween-20 (PBS-T) for 4 times. After washing with PBS-T (4  $\times$  200  $\mu\text{l}$ ), blocking solution (1% BSA in PBS) was dispensed into the wells followed by incubation for 1 h. This was followed by washing with PBS-T (4  $\times$  200  $\mu\text{l}$ ). Biotin labeled FA-MIPs or NIPs were dispensed into each well (100  $\mu\text{l}$ , 0.002  $\text{mg ml}^{-1}$ ) and incubated for 1.5 h. After washing with PBS-T (4  $\times$  200  $\mu\text{l}$ ) 100  $\mu\text{l}$  of streptavidin-conjugated HRP (1:10000 dilution) in PBS was added into each well followed by incubation for 1 h. The HRP substrate, TMB reagent (100  $\mu\text{l}$ ) was added to each well followed by incubation for 5–10 min and then the enzymatic reaction was stopped by the addition of  $\text{H}_2\text{SO}_4$  (0.5 M, 50  $\mu\text{l}$ ). The plate was then read by UV/Visible microplate reader (Epoch, Biotek) at 450 nm.

## **3. Results**

### **3.1. Purification of diphtheria toxin fragment A**

For the enzymatic digestion of DT, trypsin and trypsin-DTT were used separately and demonstrated by SDS-PAGE. Trypsin-DTT was more effective than trypsin (Figure 1a). Digested DT was injected into a fast protein liquid chromatography (FPLC) device. The peak fractions seen in the chromatogram were collected (Figure 1b). Western blot analysis was performed with the proteins in the fractions. The 1st peak fractions (36, 37, 38) had DT (full toxin) and the 2nd peak fractions (48, 49, 50) had a very large amount of FA (Figure 1c). Thus, DT digestion with trypsin + DTT was performed successfully and confirmed by SDS-PAGE, FPLC and western blot analysis.

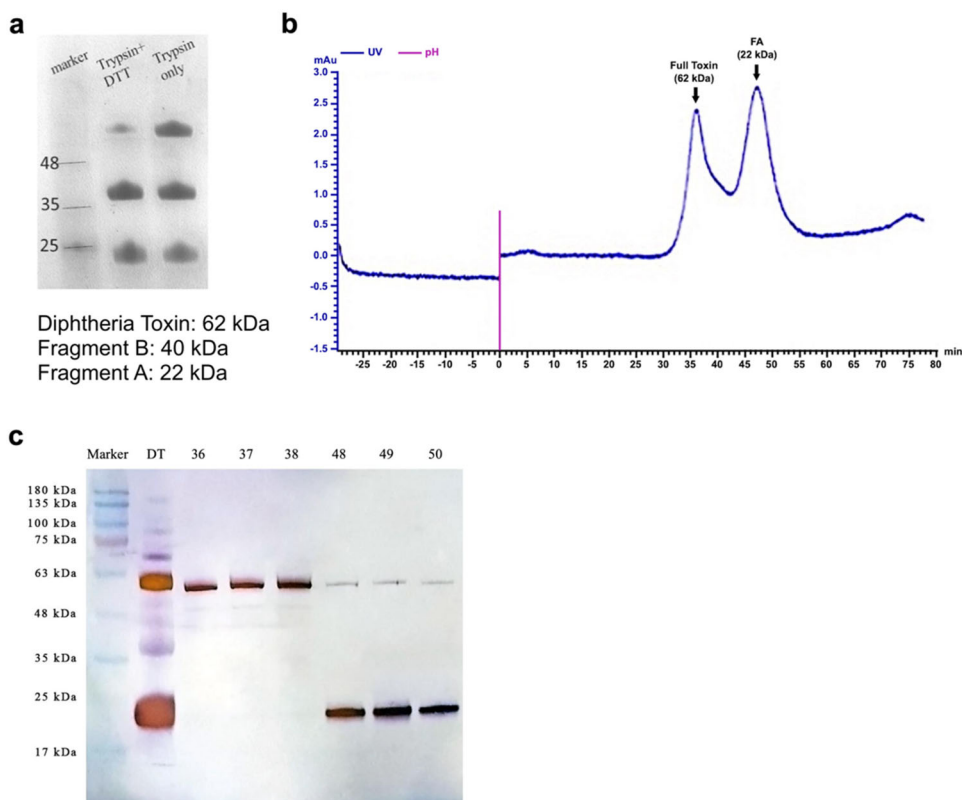


**Figure 1.** Enzymatic digestion of DT was determined by SDS-PAGE, chromatography, and western blot studies. (a) SDS-PAGE gel image of DT after digestion with trypsin and trypsin + DTT (DT (full toxin), FA and FB are seen in SDS-PAGE gel at the end of enzymatic digestion of DT). (b) Chromatogram of Full DT toxin and FA fractions of DT given to the chromatography device after digestion with trypsin + DTT (sample volume: 1 ml, flow rate: 1 ml min<sup>-1</sup>, DT concentration: 2 μg ml<sup>-1</sup>). (c) Western-Blot result using anti-FA (36–38; DT [full toxin], 48–50; FA).

### 3.2. Morphological characterization of imprinted polymer

Details for the structural characterization of the functional monomer TAPA are given in our previous paper [20]. In conventional miniemulsion polymerization, strong surfactants are required to form effective, stabilized, and small nanosized micelles. Usually, ionic surfactants such as SDS are used. PVA, a nonionic surfactant, has a long nonionic polymer chain emulsifying. The combined use of SDS and PVA has a remarkable effect on particle stability. Electrostatic repulsion between SDS molecules is associated with PVA. This causes tension in the polyol chains and simultaneously creates a very large charge area on the drop surface. The repulsive forces prevent the nanodrops from approaching each other and delay the coalescence formation. In addition, PVA is used to prevent the denaturing of the template protein in the presence of SDS and to reduce the protein-surfactant interaction.

It is common in the literature to use co-surfactant hexadecane to obtain a stable and regular particle size miniemulsion [20]. FA-MIP nanoparticles had a particle size of about 100 nm in the STEM images (Figure 2a–c). In the SEM images, tightly

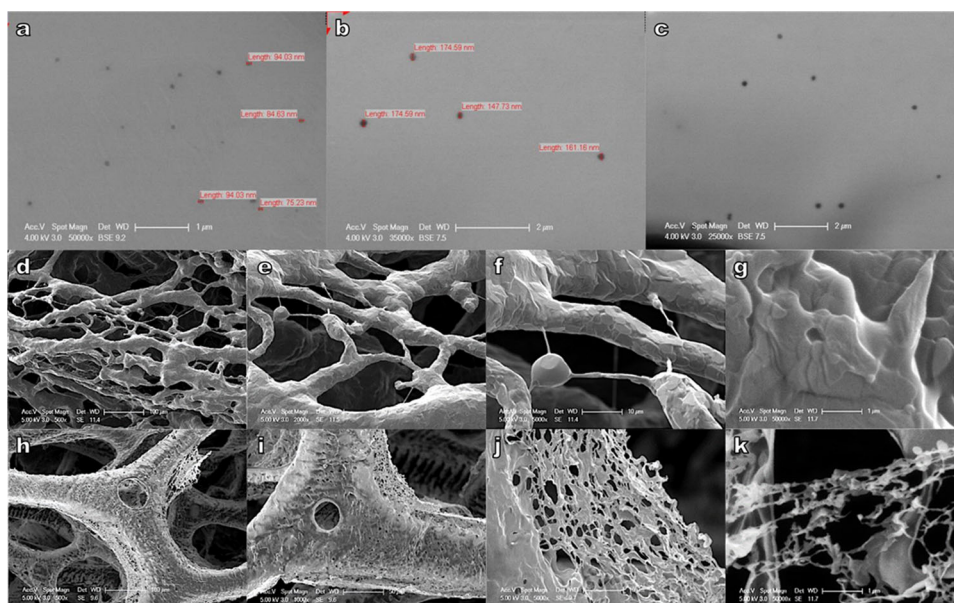


**Figure 2.** STEM and SEM images of freeze-dried cast films of FA-MIP nanoparticles before and after dialysis. (a-c) In STEM images, FA-MIP nanoparticles have a particle size of about 100 nm. (d-g) In the SEM images, tightly packed polymer chains with large pores are seen on the surface of the non-dialyzed sample (magnifications: 500x, 2000x, 5000x and 50000x). The anchored particles inside the pores are considered to be FA. (h-k) In the dialyzed sample, the porous and fibrous structure is observed demonstrating the FA removal from nanoparticles (magnifications: 500x, 1000x, 5000x and 50000x).

packed polymer chains are seen on the surface in the non-dialyzed sample (Figure 2d–g), while a porous and fibrous structure is observed in the dialyzed sample (Figure 2h–k) when diphtheria is imprinted.

### 3.3. Cytotoxicity assays

#### 3.3.1. Interactions of cells with diphtheria toxin

The cytotoxic effect of DT on HUVEC was determined by MTT assay and 500 ng ml<sup>-1</sup> DT killed approximately 50% of the cells after 24 h. In addition, cell viability of cells treated with 5, 500 and 5000 ng ml<sup>-1</sup> DT was below 25% after 48 and 72 h (Figure 3).

#### 3.3.2. Interactions of cells with non-imprinted polymer

The cytotoxic effect of NIP on HUVEC was determined by MTT assay. 1 and 10 µg ml<sup>-1</sup> NIP did not cause a significant decrease in cell viability after 24 and 48 h. Cell viability was also above 50% after 72 h (Figure 4).

### 3.4. Immunofluorescent staining

The cytotoxic effect of DT on HUVEC was visualized by immunofluorescence staining (Figure 5). 500 ng ml<sup>-1</sup> DT caused disruption of actin filaments after 24, 48 and

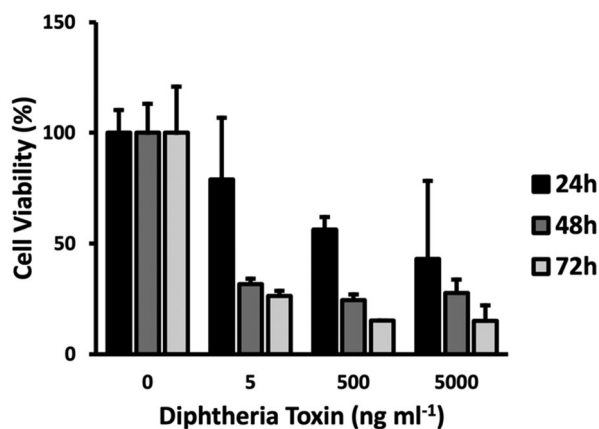


**Figure 3.** Cell viability of HUVEC treated with DT. Columns show mean values of three independent experiments ( $\pm$ SEM).

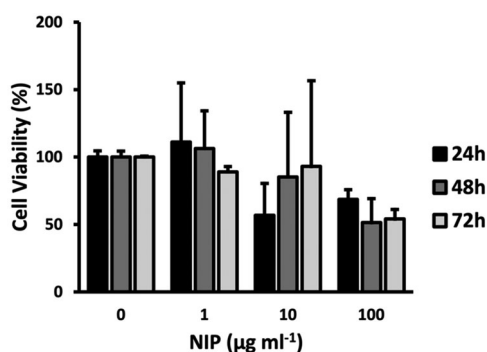


**Figure 4.** Cell viability of HUVEC treated with NIP. Columns show mean values of three independent experiments ( $\pm$ SEM).

72 h (Figure 5c–j). In particular, actin filaments were severely damaged after 72 h. Also, 5000 ng ml<sup>-1</sup> DT caused complete destruction of actin filaments after 24 h (Figure 5d).

The cytotoxic effect of NIP on HUVEC was also visualized by immunofluorescent staining. At the end of 24 and 48 h, the actin filaments of the cells were not damaged. MTT assay and immunofluorescent staining results were similar (Figure 6).

### 3.5. Neutralization tests

#### 3.5.1. Interactions of cells with molecular imprinted polymer and diphtheria toxin

The cytotoxic effect of 100 ng ml<sup>-1</sup> DT on HUVEC in the presence of FA-MIP was visualized by immunofluorescent staining. After 24 and 48 h, the actin filaments of the cells were significantly similar to the control cells (Figure 7).

Cell viability of HUVEC treated with 100 ng ml<sup>-1</sup> DT in the presence of FA-MIP was determined by MTT assay (Figure S1). After 24 h, the cytotoxic effect on HUVEC treated with 100 ng ml<sup>-1</sup> DT was neutralized in the presence of 1, 2 and 5 µg ml<sup>-1</sup> FA-MIP (Figure S2). Notably, HUVEC cell viability treated with 100 ng

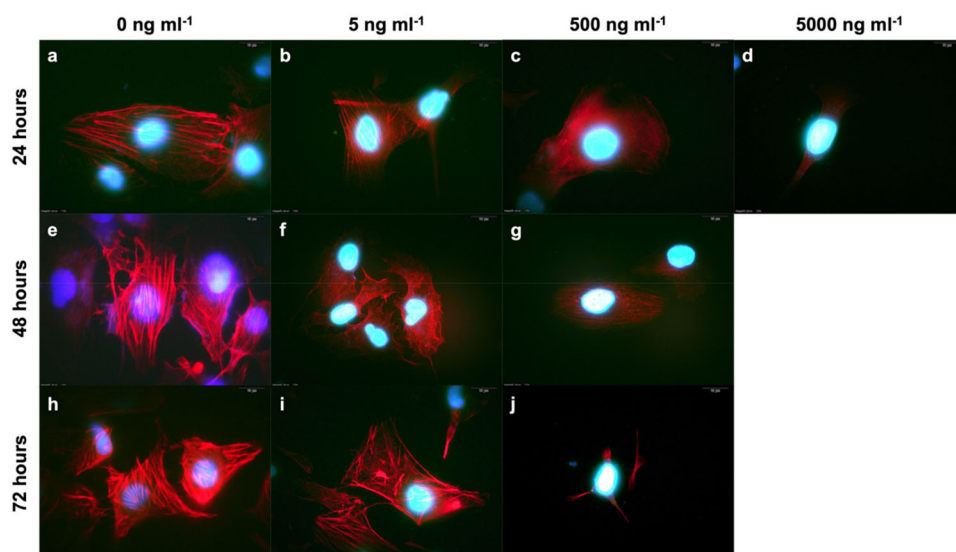


**Figure 5.** Immunofluorescent staining images of HUVEC treated with DT at  $10\ \mu\text{m}$  and  $100\times$  magnification after 24–48–72 h. For 48 and 72 h, DT concentrations of  $5000\ \text{ng ml}^{-1}$  were not included in the experiment since actin filaments lost their structural properties to a great extent at  $500\ \text{ng ml}^{-1}$  DT concentration.

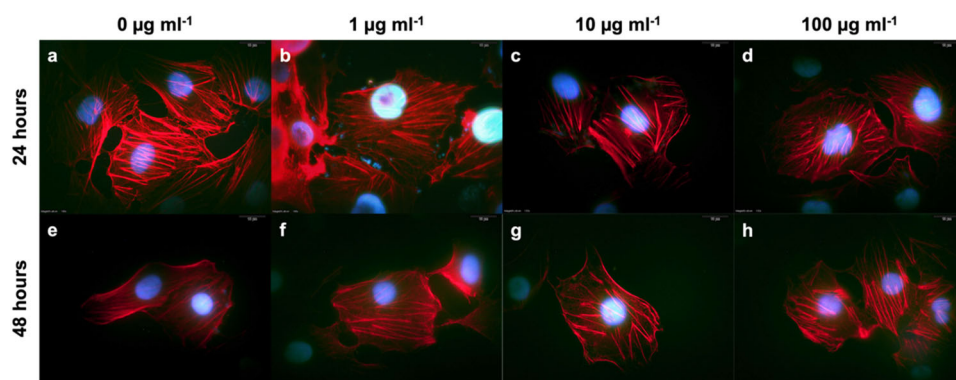


**Figure 6.** Immunofluorescent staining images of HUVEC treated with NIP at  $10\ \mu\text{m}$  and  $100\times$  magnification after 24–48 h.

$\text{ml}^{-1}$  DT in the presence of  $1\ \mu\text{g ml}^{-1}$  FA-MIP was 25.04% higher than without FA-MIP (Figure 8).

### 3.6. Binding efficiency and selectivity studies of FA-MIPs against DT

One of the purposes of this study was to use imprinted polymers in ELISA system. In order to use biotin-streptavidin interaction as a detection system first we started with the optimization of labeling NIPs with biotin. We labeled NIPs with 50, 100, 250 and  $500\ \mu\text{g}$  biotin and then removed unbound biotin with dialysis (Figure 9). There was no significant difference between biotin concentrations and a final concentration of

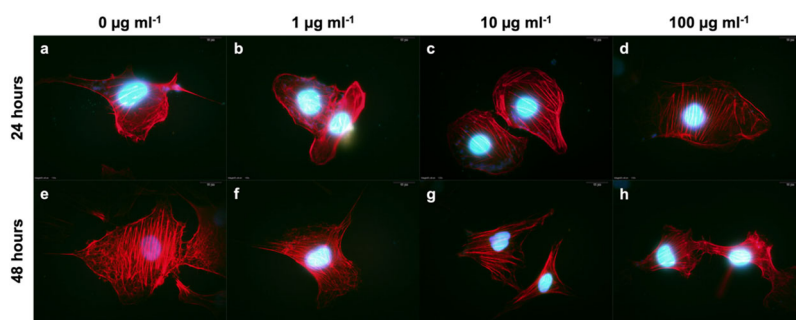


**Figure 7.** Immunofluorescent staining images of HUVEC treated with  $100 \text{ ng ml}^{-1}$  DT and 0, 1, 10,  $100 \mu\text{g ml}^{-1}$  FA-MIP at  $10 \mu\text{m}$  and  $100\times$  magnification after 24–48 h. In the presence of FA-MIP, the structure of actin filaments (red) in HUVEC was not disrupted by DT. DT: a, e:  $0 \text{ ng ml}^{-1}$ , b, c, d, f, g, h:  $100 \text{ ng ml}^{-1}$ ; FA-MIP: a:  $0 \mu\text{g ml}^{-1}$ , b:  $1 \mu\text{g ml}^{-1}$ , c:  $10 \mu\text{g ml}^{-1}$ , d:  $100 \mu\text{g ml}^{-1}$ , e:  $0 \mu\text{g ml}^{-1}$ , f:  $1 \mu\text{g ml}^{-1}$ , g:  $10 \mu\text{g ml}^{-1}$ , h:  $100 \mu\text{g ml}^{-1}$ .

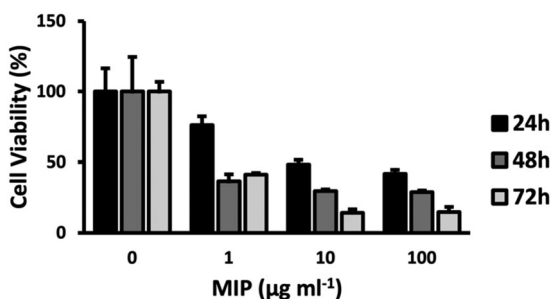


**Figure 8.** Cell viability of HUVEC treated with DT in the presence of FA-MIP. Cells were treated with  $100 \text{ ng ml}^{-1}$  DT and 1, 10 and  $100 \mu\text{g ml}^{-1}$  FA-MIP for 24, 48 and 72 h. Columns show mean values of three independent experiments ( $\pm$ SEM).

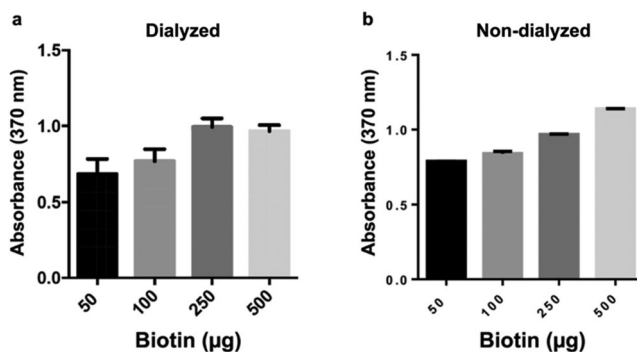


**Figure 9.** Determination of biotin-NIP interaction by ELISA method. NIPs were labeled with 50, 100, 250 and  $500 \mu\text{g}$  biotin and the absorbance values of the interactions between each other were determined. (a) dialyzed, (b) non-dialyzed. Columns show mean values of three independent experiments ( $\pm$ SEM).

$100 \mu\text{g}$  biotin was used to label NIP and FA-MIPs for DT and FA ELISA. We showed with ELISA results that FA-MIPs can bind to both whole toxin (DT) and its fragment (FA) with the same affinity (Figure 10).

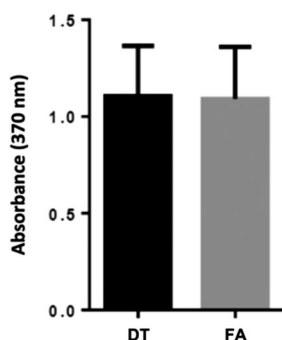


**Figure 10.** Interaction of DT and FA with FA-MIP. ELISA results showed that FA-MIPs could bind to both the whole toxin (DT) and its fragment (FA) with the same affinity. Columns show the mean values of three independent experiments ( $\pm$ SEM).

#### 4. Discussion

In this study, we determined that the FA-MIPs can bind macromolecules with selective affinity. We synthesized FA-MIP based on antibody-antigen interactions and defined it as plastic antibody.

There are two main problems encountered in the preparation of biomacromolecule imprinted materials. The first is the denaturation of proteins or peptides during the imprinting process. To avoid this problem, the reactions and imprinting process must be carried out under physiological conditions (neutral pH, aqueous medium and room temperature) [31]. The second problem is slow mass transfer. Although molecular imprinting has recently been used for biomacromolecular targets such as peptides and proteins, imprinting problems have not been completely overcome [31–33]. Therefore, there is an increasing interest for epitope imprinting approach in current studies. Shea et al. used a plastic antibody against the bee venom mellitin (26 amino acids) to treat mice infected with mellitin for the first time, adding a new dimension to molecular imprinting applications [34]. Our template molecule is DT (535 amino acids), which has a much larger molecular weight than mellitin. In another study using epitope imprinting, boronate affinity-anchored epitopes used as a template for imprinting of  $\beta$ 2-Microglobulin (B2M) containing 99 amino acids and myoglobin (Mb) containing 153 amino acids [12]. Other researchers have immobilized hemoglobin (Hb) on silica nanoparticles and then fragmented by trypsin digestion. HB-selective MIPs was synthesized by imprinting the peptides obtained by washing after digestion [10]. In our study, we preferred the miniemulsion polymerization technique by the surface imprinting method. The main reason for this choice is the miniemulsion technique is that it eliminates the problems of other conventional emulsion polymerizations such as water dissolution and transport of reactants through the aqueous phase. Moreover, during the miniemulsion polymerization reaction time, under ideal conditions, the monomer drops are small in size, homogeneous and kinetically stable.

One of the reasons we prefer DT as a template molecule is that it consists of fragments A and B, which can be separated by enzymatic digestion. From this point of view, we aimed to capture all of the DT by imprinting the FA fragment obtained by

enzymatic digestion. One of the remarkable results of this study is that the FA-MIP we developed for FA has the ability to bind whole DT. This finding shows that plastic antibodies that recognize the whole antigen molecule can be synthesized by imprinting epitopes on antigen molecules as template molecules. Thus, it will be possible to eliminate the mass transfer problem.

In summary, our data reveal that macromolecules can be imprinted by epitope approach in molecular imprinting. In addition to *in vitro* studies on the HUVEC cell line, *in vivo* studies are also needed to increase the efficiency of the plastic antibody.

## 5. Conclusion

To conclude, it was shown that FA can be used as a template molecule for the synthesis of MIP with specificity against DT. However, for certain practical applications, using epitopes as template molecules is more economically profitable than using whole biomolecules or their parts. Therefore, it is necessary to emphasize that selection of the epitope is important to insure high recognition and strong binding of macromolecules.

## Disclosure statement

No potential conflict of interest was reported by the authors.

## Funding

Financial assistance for this research by The Scientific and Technological Research Council of Turkey (TUBITAK Project No. 115S224); and The Scientific Research Projects Coordination Unit of Istanbul University (BAP Project No. 25648).

## ORCID

Süleyman Serdar Alkanlı  <http://orcid.org/0000-0003-0482-8246>

Fulya Dal Yöntem  <http://orcid.org/0000-0003-4767-083X>


Merve Yaşar  <http://orcid.org/0000-0001-7633-8823>

Celal Güven  <http://orcid.org/0000-0003-0499-7787>

M. Vezir Kahraman  <http://orcid.org/0000-0003-1043-6476>

Nilhan Kayaman Apohan  <http://orcid.org/0000-0002-7750-3058>

Zerrin Aktaş  <http://orcid.org/0000-0002-5998-0440>

Mustafa Oral Öncül  <http://orcid.org/0000-0002-1681-1866>

Ayhan Ünlü  <http://orcid.org/0000-0001-6033-7148>

Handan Akçakaya  <http://orcid.org/0000-0002-7499-6061>

## References

- [1] Zhang H. Molecularly imprinted nanoparticles for biomedical applications. *Adv Mater.* 2020;32(3):e1806328.
- [2] Zhang DD, Liu JM, Sun SM, et al. Construction of persistent luminescence-plastic antibody hybrid nanoprobe for *in vivo* recognition and clearance of pesticide using background-free nanobioimaging. *J Agric Food Chem.* 2019;67(24):6874–6883.

- [3] Chen F, Mao M, Wang J, et al. A dual-step immobilization/imprinting approach to prepare magnetic molecular imprinted polymers for selective removal of human serum albumin. *Talanta*. 2020;209:120509.
- [4] Moczko E, Guerreiro A, Cáceres C, et al. Epitope approach in molecular imprinting of antibodies. *J Chromatogr B Analyt Technol Biomed Life Sci*. 2019;1124:1–6.
- [5] Li L, Lu Y, Bie Z, et al. Photolithographic boronate affinity molecular imprinting: a general and facile approach for glycoprotein imprinting. *Angew Chem Int Ed Engl*. 2013;52(29):7451–7454.
- [6] Kryscio DR, Peppas NA. Critical review and perspective of macromolecularly imprinted polymers. *Acta Biomater*. 2012;8(2):461–473.
- [7] Verheyen E, Schillemans JP, van Wijk M, et al. Challenges for the effective molecular imprinting of proteins. *Biomaterials*. 2011;32(11):3008–3020.
- [8] Whitcombe MJ, Chianella I, Larcombe L, et al. The rational development of molecularly imprinted polymer-based sensors for protein detection. *Chem Soc Rev*. 2011;40(3):1547–1571.
- [9] Ertürk G, Mattiasson B. Molecular imprinting techniques used for the preparation of biosensors. *Sensors (Basel)*. 2017;17(2):288.
- [10] Pasquardini L, Bossi AM. Molecularly imprinted polymers by epitope imprinting: a journey from molecular interactions to the available bioinformatics resources to scout for epitope templates. *Anal Bioanal Chem*. 2021;413(24):6101–6115.
- [11] Chou CY, Lin CY, Wu CH, et al. Sensing HIV protease and its inhibitor using “helical epitope”-imprinted polymers. *Sensors (Basel)*. 2020;20(12):3592.
- [12] Xing R, Ma Y, Wang Y, et al. Specific recognition of proteins and peptides via controllable oriented surface imprinting of boronate affinity-anchored epitopes. *Chem Sci*. 2019;10(6):1831–1835.
- [13] Bennett MJ, Choe S, Eisenberg D. Refined structure of dimeric diphtheria toxin at 2.0 Å resolution. *Protein Sci*. 1994;3(9):1444–1463.
- [14] Murphy JR. Mechanism of diphtheria toxin catalytic domain delivery to the eukaryotic cell cytosol and the cellular factors that directly participate in the process. *Toxins (Basel)*. 2011;3(3):294–308.
- [15] Flores-Canales J, Vargas-Urbe M, Ladokhin A, et al. Membrane association of the diphtheria toxin translocation domain studied by coarse-grained simulations and experiment. *J Membr Biol*. 2015;248(3):529–543.
- [16] Oh KJ, Senzel L, Collier RJ, et al. Translocation of the catalytic domain of diphtheria toxin across planar phospholipid bilayers by its own T domain. *Proc Natl Acad Sci U S A*. 1999;96(15):8467–8470.
- [17] Bras M, Queenan B, Susin SA. Programmed cell death via mitochondria: different modes of dying. *Biochemistry (Mosc)*. 2005;70(2):231–239.
- [18] Bektaş M, Varol B, Nurten R, et al. Interaction of diphtheria toxin (fragment A) with actin. *Cell Biochem Funct*. 2009;27(7):430–439.
- [19] Schnell L, Mittler AK, Mattarei A, et al. Semicarbazone EGA inhibits uptake of diphtheria toxin into human cells and protects cells from intoxication. *Toxins (Basel)*. 2016;8(7):221.
- [20] Yaşar M, Yöntem FD, Kahraman MV, et al. Polymeric nanoparticles for selective protein recognition by using thiol-ene miniemulsion photopolymerization. *J Biomater Sci Polym Ed*. 2020;31(16):2044–2059.
- [21] Taskin E, Guven C, Kaya ST, et al. The role of toll-like receptors in the protective effect of melatonin against doxorubicin-induced pancreatic beta cell toxicity. *Life Sci*. 2019;233:116704.
- [22] Früh A, Tielking K, Schoknecht F, et al. RNase A inhibits formation of neutrophil extracellular traps in subarachnoid hemorrhage. *Front Physiol*. 2021;12:724611.
- [23] Eggers B, Marciniak J, Memmert S, et al. Influences of cold atmospheric plasma on apoptosis related molecules in osteoblast-like cells in vitro. *Head Face Med*. 2021;17(1):37.

- [24] Collier RJ. Diphtheria toxin: mode of action and structure. *Bacteriol Rev.* 1975;39(1): 54–85.
- [25] Collier RJ, Kandel J. Structure and activity of diphtheria toxin. I. Thiol-dependent dissociation of a fraction of toxin into enzymically active and inactive fragments. *J Biol Chem.* 1971;246(5):1496–1503.
- [26] Drazin R, Kandel J, Collier RJ. Structure and activity of diphtheria toxin. II. Attack by trypsin at a specific site within the intact toxin molecule. *J Biol Chem.* 1971;246(5): 1504–1510.
- [27] Özerman EB, Varol B, Hacısmanoğlu E, et al. Cross-reacting material 197 (CRM197) affects actin cytoskeleton of endothelial cells. *Gen Physiol Biophys.* 2017;36(4):383–389.
- [28] Laemmli UK. Cleavage of structural proteins during the assembly of the head of bacteriophage T4. *Nature.* 1970;227(5259):680–685.
- [29] Landfester K, Mailänder V. Nanocapsules with specific targeting and release properties using miniemulsion polymerization. *Expert Opin Drug Deliv.* 2013;10(5):593–609.
- [30] EZ-Link Sulfo-NHS-LC-Biotin [Internet]. Rockford (IL): Thermo Scientific; [cited 2018]. Available from: <https://www.fishersci.co.uk/shop/products/ez-link-sulfo-nhs-lc-biotin-labeling-kits/10538723>.
- [31] Hoshino Y, Kodama T, Okahata Y, et al. Peptide imprinted polymer nanoparticles: a plastic antibody. *J Am Chem Soc.* 2008;130(46):15242–15243.
- [32] Li MX, Wang XH, Zhang LM, et al. A high sensitive epitope imprinted electrochemical sensor for bovine serum albumin based on enzyme amplifying. *Anal Biochem.* 2017; 530:68–74.
- [33] Tan CJ, Chua HG, Ker KH, et al. Preparation of bovine serum albumin surface-imprinted submicrometer particles with magnetic susceptibility through core-shell mini-emulsion polymerization. *Anal Chem.* 2008;80(3):683–692.
- [34] Hoshino Y, Koide H, Urakami T, et al. Recognition, neutralization, and clearance of target peptides in the bloodstream of living mice by molecularly imprinted polymer nanoparticles: a plastic antibody. *J Am Chem Soc.* 2010;132(19):6644–6645.